

**Predictive approach of SEU occurrence induced by neutron in SRAM and EEPROM\***

JIN Xiao-Ming (金晓明),<sup>†</sup> YANG Shan-Chao (杨善潮), LI Da (李达),  
 ZHANG Wen-Shou (张文首), WANG Chen-Hui (王晨辉), LI Rui-Bin (李瑞宾),  
 WANG Gui-Zhen (王桂珍), BAI Xiao-Yan (白小燕), QI Chao (齐超), and LIU Yan (刘岩)  
*State Key Laboratory of Intense Pulsed Radiation Simulation and Effect,  
 Northwest Institute of Nuclear Technology, Xi'an 710024, China*

(Received January 13, 2015; accepted in revised form June 11, 2015; published online October 20, 2015)

A simulation approach is developed to obtain the linear energy transfer (LET) spectrum of all secondary ions and predict single event upset (SEU) occurrence induced by neutron in memory devices. Neutron reaction channels, secondary ion species and energy ranges, and LET calculation method are introduced respectively. Experimental results of neutron induced SEU effects on static random access memory (SRAM) and programmable read only memory (EEPROM) are presented to confirm the validity of the simulation results.

Keywords: Neutron radiation, Memory device, Single event upset (SEU), Linear energy transfer (LET)

DOI: [10.13538/j.1001-8042/nst.26.050501](https://doi.org/10.13538/j.1001-8042/nst.26.050501)

**I. INTRODUCTION**

Single event upset (SEU) induced by neutrons in advanced memory devices is currently recognized as one of the major concerns in issues of reliability [1–4]. Although neutrons are uncharged particles and can't directly induce electron-hole pairs in semiconductor devices, they transfer energy and produce recoil and spallation products that are highly ionizing and therefore capable of creating electron-hole pairs in semiconductor materials [5, 6]. Secondary ions, such as recoil and spallation products, can create large numbers of excess carriers and possibly cause SEU in memory devices. Previous literature reports the phenomenon and mechanism of SEU [7, 8]. Experiments show that neutron induced SEU has been identified in memory devices and the cross sections for various memory devices are measured in different neutron radiation environments [9]. Simulation of neutron induced SEU effects is mainly based on the Monte Carlo method, as this method is useful for simulating SEU of a memory chip induced by neutrons and providing a detailed description of the random processes of SEU. Li H's paper provides a Monte Carlo method to simulate the process of energy deposition in sensitive volumes and to calculate the SEU cross-section [10]. In addition, as one of the Monte Carlo toolkits, Geant4, is currently playing a more and more important role in many nuclear technology applications, and is especially used for neutron transport and nuclear reaction simulation. In Pete Truscott's paper, Geant4 is performed to simulate neutron SEU effects. SEU rate predictions are in good agreement with experimental data for large ( $\sim 300\ \mu\text{m}$ ) to small ( $\sim 0.5\ \mu\text{m}$ ) feature-size devices [11]. All the above-mentioned research provides a universal understanding of neutron induced SEU effects, and demonstrates that the Monte Carlo method, such as Geant4, is a reasonable and effective approach for neutron SEU simulation.

However, few research papers focus on how to predict the occurrence of SEU for different kinds of memory devices in neutron radiation fields. Practical neutron radiation, such as the reactor neutron, terrestrial neutron, and atmosphere neutron, provides both thermal and fast neutrons over a wide range of energies. In this paper, the experiments are performed at the Xi'an pulsed reactor (XAPR) at the state key laboratory of intense pulsed radiation simulation and effect in China, so in the simulation the incident neutron spectrum is the XAPR neutron spectrum. Because of the complicated device structure and neutron spectrum, it is quite challenging to determine whether memory devices exhibit SEU effect in the neutron radiation environment.

It is a well known fact that linear energy transfer (LET), referring to energy loss of an incident ion per unit length in material, is an important parameter in detailed analysis of the SEU effect. It is commonly presumed that SEU occurs whenever the LET of ions is more than the SEU threshold of the memory device. According to this knowledge, it is of the essence to calculate the LET range of all secondary ions induced by the neutron. In this paper, the objective is to predict whether SEU occurs in certain memory devices exposed to neutron radiation. First of all, in order to determine the energy spectra of each secondary ion induced by the neutron, the Geant4 Monte-Carlo simulation program is adopted to process the transport of neutrons in silicon dioxide and simulate the interaction between incident neutrons and target atoms. Secondly, the LET of secondary ions is calculated using Stopping and Ranges of Ions in Matter (SRIM). Thus SEU will occur when the maximum LET is more than the SEU threshold of a memory device, and vice versa. Finally, reactor neutron radiation experiments on static random access memory (SRAM) and programmable read only memory (EEPROM) are performed to confirm the simulation prediction.

**II. SIMULATION PROCEDURE**

In our simulation, in order to predict the occurrence of SEU induced by neutrons in silicon-based memory devices,

\* Supported by National Natural Science Foundation of China (No. 11235008)

<sup>†</sup> Corresponding author, [jinxiaoming@nint.ac.cn](mailto:jinxiaoming@nint.ac.cn)

the problem is to calculate the LET spectrum of all secondary ions, considering the incident neutron spectrum, target material, and nuclear reaction channels. The incident neutron spectrum defines the primary neutron energy in the simulation by Monte Carlo random sample. The target material is defined as silicon dioxide. The top layer materials, such as copper, are not considered in the simulation for two reasons. The first is that in silicon-based devices, silicon dioxide is the major material for insulation and isolation of adjacent transistors, while other layer materials are minor. The second is that the sensitive volume material is silicon, so the reactions between the sensitive volume material and neutron can be included in the reactions between silicon dioxide and the neutron. For the reactions between the neutron and silicon dioxide, there are 30 comprehensive nuclear reaction channels, as shown in Table 1.

For analysis presented within this paper, the prediction simulation is primarily based on the Geant4 and SRIM simulation toolkits. Type and energy distribution of secondary ions, which are exported from the Geant4 simulation, are imported into SRIM to calculate the LET value of each secondary ion.

Geant4 uses the NeutronHP model for neutron interactions from thermal energies up to 20 MeV. In this paper, the Geant4 Monte-Carlo program is first adopted to deal with collision, moderation, and nuclear reaction, and simulate the energy distribution of secondary ions produced from the nuclear reaction. The initial neutron energy spectrum, physical process, and reaction channels should be taken into consideration. Figure 1 shows the initial neutron spectrum provided by XAPR. In the Geant4 primary generator action file, the primary energy of the incident neutron is sampled from the spectrum mentioned above by random sampling. The neutron energy ranges from  $3.6 \times 10^{-3}$  eV to 20 MeV. The majority of neutrons are in the low energy range, and differential flux decreases with an increase in neutron energy after 10 eV. In Geant4, neutron transport at energies below 20 MeV is based on empirical elastic and inelastic neutron cross-section data drawn from many of the standard database sources [12]. Ionization due to the recoil nucleus and secondary charged nucleons includes accurate treatment of low-energy electromagnetic processes, using electronic stopping power for protons and  $\alpha$  particles, multiple scattering, and  $\delta$ -ray production from ions [13].

In silicon based semiconductor devices, when the initial neutron is passing through a sensitive region, the neutron interacts with nuclei from the device material, predominantly  $^{28}\text{Si}$  and  $^{16}\text{O}$ . The reaction is elastic when conserving momentum, or inelastic when the neutron is absorbed followed by an ejection of nuclear fragments. The characteristics (ion type and energy) of the secondary ions responsible for SEU strongly depend on the type of nuclear reaction [14]. As shown in Table 1, the various nuclear reactions can only occur above a certain energy threshold of a few MeV. As neutron energy increases, the number of reaction channels increases. Consequently, neutrons with low energy will not be very efficient in creating SEU effects through limited reactions. For neutrons above 17.8 MeV, all of the reaction chan-

TABLE 1. Schematic of neutron reaction channels and associated threshold energies

| Serial number | Reaction channels                           | Neutron threshold energy |
|---------------|---|--------------------------|
| 1             | $^{28}\text{Si}(n,2n)^{27}\text{Si}$        | $n > 17.8 \text{ MeV}$   |
| 2             | $^{28}\text{Si}(n,n\alpha)^{24}\text{Mg}$   | $n > 10.4 \text{ MeV}$   |
| 3             | $^{28}\text{Si}(n,n)^{28\text{m}}\text{Si}$ | $n > 1.8 \text{ MeV}$    |
| 4             | $^{28}\text{Si}(n,g)^{29}\text{Si}$         | 0                        |
| 5             | $^{28}\text{Si}(n,p)^{28}\text{Al}$         | $n > 4 \text{ MeV}$      |
| 6             | $^{28}\text{Si}(n,d)^{27}\text{Al}$         | $n > 10 \text{ MeV}$     |
| 7             | $^{28}\text{Si}(n,\alpha)^{25}\text{Mg}$    | $n > 2.7 \text{ MeV}$    |
| 8             | $^{29}\text{Si}(n,2n)^{28}\text{Si}$        | $n > 8.8 \text{ MeV}$    |
| 9             | $^{29}\text{Si}(n,n\alpha)^{25}\text{Mg}$   | $n > 11.5 \text{ MeV}$   |
| 10            | $^{29}\text{Si}(n,np)^{28}\text{Al}$        | $n > 12.3 \text{ MeV}$   |
| 11            | $^{29}\text{Si}(n,n)^{29\text{m}}\text{Si}$ | $n > 1.3 \text{ MeV}$    |
| 12            | $^{29}\text{Si}(n,g)^{30}\text{Si}$         | 0                        |
| 13            | $^{29}\text{Si}(n,p)^{29}\text{Al}$         | $n > 3 \text{ MeV}$      |
| 14            | $^{29}\text{Si}(n,\alpha)^{26}\text{Mg}$    | $n > 1.3 \text{ MeV}$    |
| 15            | $^{30}\text{Si}(n,2n)^{29}\text{Si}$        | $n > 11 \text{ MeV}$     |
| 16            | $^{30}\text{Si}(n,n\alpha)^{26}\text{Mg}$   | $n > 12 \text{ MeV}$     |
| 17            | $^{30}\text{Si}(n,np)^{29}\text{Al}$        | $n > 14 \text{ MeV}$     |
| 18            | $^{30}\text{Si}(n,n)^{30\text{m}}\text{Si}$ | $n > 2.3 \text{ MeV}$    |
| 19            | $^{30}\text{Si}(n,g)^{31}\text{Si}$         | $n > 1.5 \text{ MeV}$    |
| 20            | $^{30}\text{Si}(n,p)^{30}\text{Al}$         | $n > 8 \text{ MeV}$      |
| 21            | $^{30}\text{Si}(n,\alpha)^{27}\text{Mg}$    | $n > 4 \text{ MeV}$      |
| 22            | $^{16}\text{O}(n,2n)^{15}\text{O}$          | $n > 17 \text{ MeV}$     |
| 23            | $^{16}\text{O}(n,n\alpha)^{12}\text{C}$     | $n > 8.5 \text{ MeV}$    |
| 24            | $^{16}\text{O}(n,np)^{15}\text{N}$          | $n > 13 \text{ MeV}$     |
| 25            | $^{16}\text{O}(n,n)^{16\text{m}}\text{O}$   | $n > 6.5 \text{ MeV}$    |
| 26            | $^{16}\text{O}(n,g)^{17}\text{O}$           | 0                        |
| 27            | $^{16}\text{O}(n,p)^{16}\text{N}$           | $n > 10 \text{ MeV}$     |
| 28            | $^{16}\text{O}(n,\alpha)^{13}\text{C}$      | $n > 4 \text{ MeV}$      |
| 29            | $^{16}\text{O}(n,d)^{15}\text{N}$           | $n > 10 \text{ MeV}$     |
| 30            | $^{16}\text{O}(n,t)^{14}\text{N}$           | $n > 17 \text{ MeV}$     |

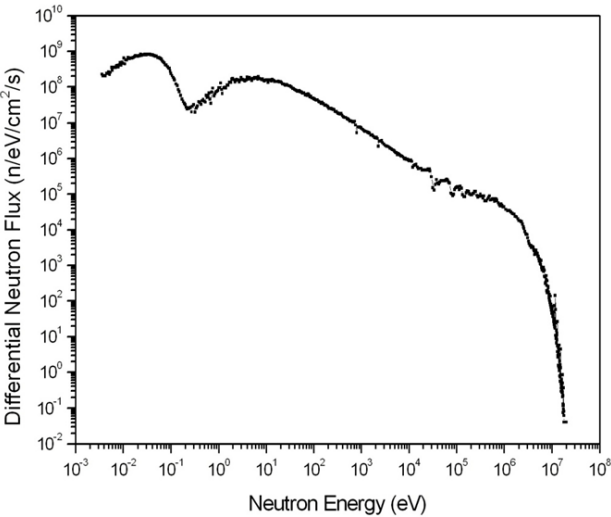


Fig. 1. Reactor neutron spectrum at XAPR.

nels are open, increasing the probability of generating a secondary ion able to induce a bit upset.

The Monte Carlo simulation code named SRIM (formerly

TRIM) is a collection of software packages developed by Ziegler and Biersack, which is written to permit the calculation of ion deposition profiles in materials exposed to energetic beams of ions [15, 16]. SRIM tables of LET, stopping power, and projected range versus ion energy are especially useful for computation of ion transport in a wide range of simulation applications. In this paper, SRIM is used to calculate the LET value of secondary ions based on ion stopping and range tables. In the LET calculation, atomic number, mass number and energy of the incident ion, and type of target material should be defined. Figure 2 shows the LET of eight types of ions, which are secondary ions of neutron reactions with Si and O atoms. In silicon, the energy to create a pair of electron-holes is 3.6 eV. Therefore, 1 MeV cm<sup>2</sup>/mg LET produces about 10.3 fC/μm of silicon. As shown in the figure, the LET of each ion increases as the energy increases initially and decreases afterwards, and the ion with a larger atomic number can evidently induce a larger LET.

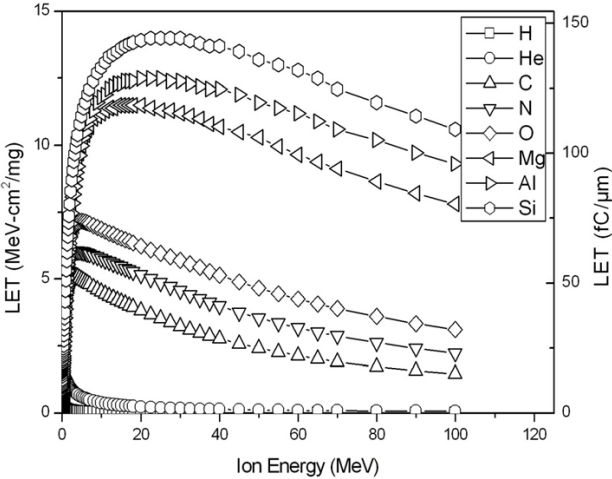


Fig. 2. (Color online) LET versus energy for eight types of secondary ions. These plots were generated using SRIM.

The simulation results of the energy range and maximum LET are shown in Table 2. The energy range of each secondary ion is simulated by Geant4, and maximum LET is calculated by SRIM. The maximum LET of neutron induced secondary ions is 9.28 MeV cm<sup>2</sup>/mg, which is caused by <sup>24</sup>Mg at 3.79 MeV. It should be noted that the maximum LET for protons and α particles in silicon is, respectively, 0.54 and 1.45 MeV cm<sup>2</sup>/mg. In addition, the SEU cross section of these particles is smaller than most of the other secondary ions. By dividing the LET range into successive intervals and calculating the proportion of ion numbers in every LET interval, we can obtain the LET spectrum of neutron induced secondary ions, as shown in Fig. 3. The LET is mostly distributed from 0 to 3 MeV cm<sup>2</sup>/mg. The peak point at 0.4 MeV cm<sup>2</sup>/mg is mainly caused by secondary low energy <sup>16</sup>O, generated from the reaction of the primary neutron with material oxygen atoms. The LET spectrum is highly useful for predicting the SEU occurrence and further investigating ionizing effect on the electrical response of the memory cell. In this paper, LET simulation results are used to

TABLE 2. The energy and maximum LET of secondary ions induced by reactor neutron

| Ion species      | Energy (keV) | Maximum LET (MeV cm <sup>2</sup> /mg) |
|------------------|--------------|---------------------------------------|
| <sup>28</sup> Si | 0–2080       | 8.16                                  |
| <sup>29</sup> Si | 0–810        | 4.49                                  |
| <sup>30</sup> Si | 0–1360       | 6.19                                  |
| <sup>31</sup> Si | 0–10         | 2.20                                  |
| <sup>27</sup> Al | 0–2130       | 7.01                                  |
| <sup>28</sup> Al | 0–1930       | 6.52                                  |
| <sup>30</sup> Al | 0–870        | 3.83                                  |
| <sup>24</sup> Mg | 0–3790       | 9.28                                  |
| <sup>25</sup> Mg | 0–3840       | 9.18                                  |
| <sup>26</sup> Mg | 0–3460       | 8.70                                  |
| <sup>27</sup> Mg | 0–2460       | 7.31                                  |
| <sup>16</sup> O  | 0–3190       | 7.04                                  |
| <sup>17</sup> O  | 0–1510       | 5.61                                  |
| <sup>14</sup> N  | 0–10         | 1.03                                  |
| <sup>15</sup> N  | 0–2820       | 5.98                                  |
| <sup>16</sup> N  | 0–2310       | 5.81                                  |
| <sup>12</sup> C  | 0–4990       | 5.14                                  |
| <sup>13</sup> C  | 0–5000       | 5.14                                  |

judge whether SEU will occur by comparing the maximum LET and the threshold of the memory device.

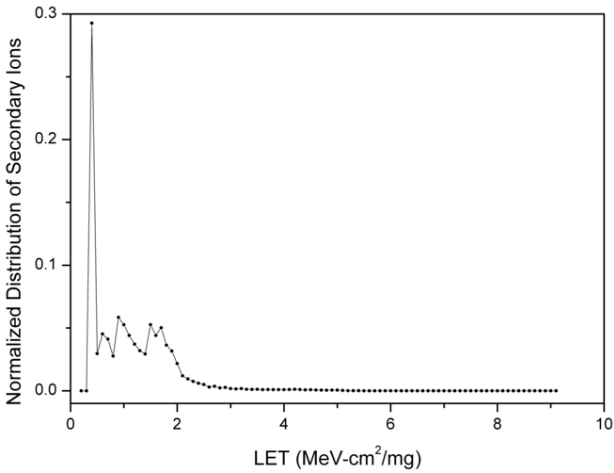


Fig. 3. LET spectrum of neutron induced secondary ions, which can be used to estimate SEU rates.

Previous literature shows that the SEU threshold is 0.3–0.7 MeV cm<sup>2</sup>/mg for CMOS SRAM with a feature size of 0.18–0.5 μm, while the maximum LET is calculated to be 9.28 MeV cm<sup>2</sup>/mg in the reactor neutron radiation environment [17, 18]. For this reason, it can be confirmed that SEU will occur in SRAM exposed to reactor neutron radiation. Previous research shows that the SEU threshold is approximately 37 MeV cm<sup>2</sup>/mg for EEPROM 28LV010, and is much larger than the maximum LET induced by the neutron [19]. Therefore, it can be confirmed that the reactor neutron will induce no SEU in the EEPROM devices with similar technological processes.

### III. EXPERIMENTAL PROCEDURE

Neutron SEU experiments were performed at XAPR. The nuclear reactor facility is located at the Northwest Institute of Nuclear Technology (NINT) in China, and provides both thermal and fast neutron beams over a range of energies. Neutron fluence was approximately  $1.0 \times 10^{14} \text{ n/cm}^2$ . The devices under test (DUTs) were SRAM and EEPROM memories. Test data transfer was carried out via USB connection to a personal computer. The test system allowed for rapid detection and storage of SEU events. Before radiation, 55 HEX (01010101) was written in each storage cell for the DUTs. During radiation, the DUTs were read continuously and the SEU test could be easily handled by the error detection and record system.

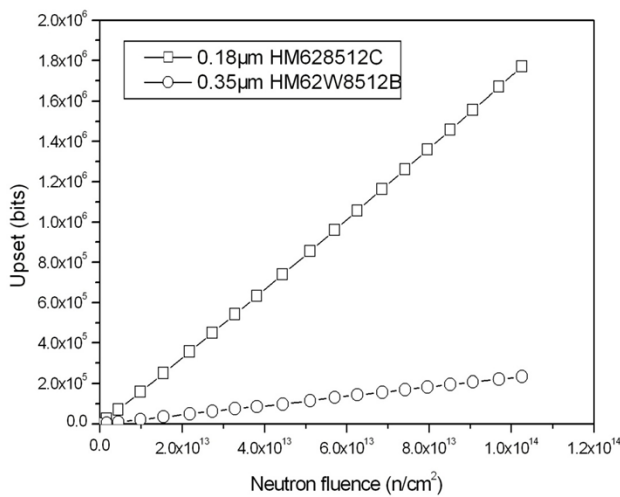


Fig. 4. Cumulative SEUs versus neutron fluence for HM62W8512B and HM628512C.

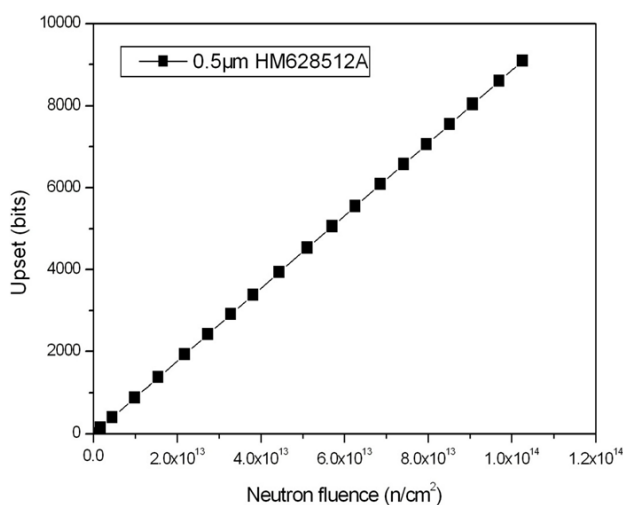


Fig. 5. Cumulative SEUs versus neutron fluence for HM628512A.

Simulation results predict that SEU for SRAM will occur in a reactor neutron environment. The experimental results are consistent with the prediction. Figure 4 shows single bit upsets induced by neutron irradiation for Hitachi HM628512C and HM62W8512B. Because of a much lower number of SEUs recorded under irradiation for Hitachi HM628512A, results for this memory are depicted separately, in Fig. 5. The SEU occurs once SRAM is exposed to neutron irradiation. In addition, the number of upsets increases linearly with neutron fluence. The SEU cross section is finally estimated from the following formula:

$$\sigma = \frac{N}{N_0 \times \phi}, \quad (1)$$

where  $N_0$  is total bit number of the SRAM block and is equal to  $2^{19}$  bits,  $N$  is number of upsets,  $\phi$  is neutron fluence, and  $N/\phi$  is equal to the slope of zero-crossing linear fitting.

The cross section is  $3.3 \times 10^{-14} \text{ cm}^2/\text{bit}$  for  $0.18 \mu\text{m}$  SRAM HM628512C,  $4.4 \times 10^{-15} \text{ cm}^2/\text{bit}$  for  $0.35 \mu\text{m}$  SRAM HM62W8512B, and  $1.7 \times 10^{-16} \text{ cm}^2/\text{bit}$  for  $0.5 \mu\text{m}$  SRAM HM628512A. As shown in the figure, the total SEUs of the HM628512C reached  $1.7 \times 10^6$  at the end of irradiation, reflecting extremely high sensitivity to reactor neutrons. The HM628512C shows greater sensitivity than HM62W8512B and HM628512A. The reason is that smaller feature size sharply increases the upset cross section by lowering the critical charges of memory cells.

Simulation results predict SEU for EEPROM is impossible in reactor neutron environments. SEU tests of EEPROM AT28C256 and AT28C040 were carried out in the neutron radiation environment. As expected, neutron radiation induced SEU effects were not significant for EEPROM while performing read operations during irradiation, since no error bit was observed in lengthy validation tests during irradiation.

### IV. CONCLUSION

A simulation approach is presented to predict SEU occurrence induced by neutrons in memory devices. The simulation is adept at processing neutron transport in semiconductor materials, obtaining type and energy distribution of secondary ions, and calculating LET values. The whole simulation procedure provides an approach to get the energy distribution and LET spectrum of neutron induced secondary ions, and introduces an applied method to predict whether SEU will occur through comparing the SEU threshold of a memory device with the maximum LET in a neutron radiation field, when the device is exposed to neutron irradiation with a complex spectrum. The experimental results show three types of SRAM devices exhibit high sensitivity to SEU effects, while two types of EEPROM devices exhibit no SEU effects. A good agreement is obtained between experimental results and simulation prediction. For hardness assurance, SEU effects must be taken into account when the maximum LET in the radiation environment exceeds the SEU threshold of the memory devices.

- [1] Haran A, Barak J, Weissman L, *et al.* 14 MeV neutrons SEU cross sections in deep submicron devices calculated using heavy ion SEU cross sections. *IEEE Trans Nucl Sci*, 2011, **58**: 848–854. DOI: [10.1109/TNS.2011.2132803](https://doi.org/10.1109/TNS.2011.2132803)
- [2] Lambert D, Baggio J, Ferlet-Cavrois F, *et al.* Neutron-induced SEU in bulk SRAMs in terrestrial environment: simulations and experiments. *IEEE Trans Nucl Sci*, 2004, **51**: 3435–3441. DOI: [10.1109/TNS.2004.839133](https://doi.org/10.1109/TNS.2004.839133)
- [3] Armani J M, Simon G and Poirot P. Low-energy neutron sensitivity of recent generation SRAMs. *IEEE Trans Nucl Sci*, 2004, **51**: 2811–2816. DOI: [10.1109/TNS.2004.835080](https://doi.org/10.1109/TNS.2004.835080)
- [4] Granlund T and Olsson N. A comparative study between proton and neutron induced SEUs in SRAMs. *IEEE Trans Nucl Sci*, 2006, **53**: 1871–1875. DOI: [10.1109/TNS.2006.880931](https://doi.org/10.1109/TNS.2006.880931)
- [5] Wrobel F, Palau J M, Calvet M C, *et al.* Incidence of multi-particle events on soft error rates caused by n-Si nuclear reactions. *IEEE Trans Nucl Sci*, 2000, **47**: 2580–2585. DOI: [10.1109/23.903812](https://doi.org/10.1109/23.903812)
- [6] Wrobel F, Palau J M, Calvet M C, *et al.* Contribution of SiO<sub>2</sub> in neutron-induced SEU in SRAMs. *IEEE Trans Nucl Sci*, 2003, **50**: 2055–2059. DOI: [10.1109/TNS.2003.821596](https://doi.org/10.1109/TNS.2003.821596)
- [7] Bagatin M, Gerardin S, Cellere G, *et al.* Annealing of heavy-ion induced floating gate errors: LET and feature size dependence. *IEEE Trans Nucl Sci*, 2010, **57**: 1835–1841. DOI: [10.1109/TNS.2010.2045131](https://doi.org/10.1109/TNS.2010.2045131)
- [8] Palau J M, Wrobel F, Castellani-Coulié K, *et al.* Monte Carlo exploration of neutron-induced SEU-sensitive volumes in SRAMs. *IEEE Trans Nucl Sci*, 2002, **49**: 3075–3081. DOI: [10.1109/TNS.2002.805420](https://doi.org/10.1109/TNS.2002.805420)
- [9] Hands A, Morris P, Dyer C, *et al.* Single event effects in power MOSFETs and SRAMs due to 3 MeV, 14 MeV and fission neutrons. *IEEE Trans Nucl Sci*, 2011, **58**: 952–959. DOI: [10.1109/TNS.2011.2106142](https://doi.org/10.1109/TNS.2011.2106142)
- [10] Li H, Deng J Y and Chang D M. Monte Carlo calculation of the cross-section of single event upset induced by 14 MeV neutrons. *Radiat Meas*, 2005, **39**: 401–407. DOI: [10.1016/j.radmeas.2004.05.005](https://doi.org/10.1016/j.radmeas.2004.05.005)
- [11] Truscott P, Lei F, Dyer C S, *et al.* Assessment of neutron- and proton-induced nuclear interaction and ionization models in Geant4 for simulating single event effects. *IEEE Trans Nucl Sci*, 2004, **51**: 3369–3374. DOI: [10.1109/TNS.2004.839517](https://doi.org/10.1109/TNS.2004.839517)
- [12] Agostinelli S, Allison J, Amako K, *et al.* Geant4—a simulation toolkit. *Nucl Instrum Meth A*, 2003, **506**: 250–303. DOI: [10.1016/S0168-9002\(03\)01368-8](https://doi.org/10.1016/S0168-9002(03)01368-8)
- [13] Truscott P, Dyer C, Frydland A, *et al.* Neutron energy-deposition spectra measurements, and comparisons with Geant4 predictions. *IEEE Trans Nucl Sci*, 2006, **53**: 1883–1889. DOI: [10.1109/TNS.2006.880936](https://doi.org/10.1109/TNS.2006.880936)
- [14] Baggio J, Lambert D, Ferlet-Cavrois V, *et al.* Single event upsets induced by 1–10 MeV neutrons in static-RAMs using mono-energetic neutron sources. *IEEE Trans Nucl Sci*, 2007, **54**: 2149–2155. DOI: [10.1109/TNS.2007.910039](https://doi.org/10.1109/TNS.2007.910039)
- [15] Ziegler J F, Ziegler M D and Biersack J P. SRIM—The stopping and range of ions in matter (2010). *Nucl Instrum Meth B*, 2010, **268**: 1818–1823. DOI: [10.1016/j.nimb.2010.02.091](https://doi.org/10.1016/j.nimb.2010.02.091)
- [16] Ziegler J F. SRIM-2003. *Nucl Instrum Meth B*, 2004, **219**: 1027–1036. DOI: [10.1016/j.nimb.2004.01.208](https://doi.org/10.1016/j.nimb.2004.01.208)
- [17] Haddad N, Rockett L, Doyle S, *et al.* Design considerations for next generation radiation hardened SRAMs for space applications. *IEEE Aerospace Conference*, 2005, 1–6. DOI: [10.1109/AERO.2005.1559542](https://doi.org/10.1109/AERO.2005.1559542)
- [18] Liu Z, Sun Y J, Li S Q, *et al.* Circuit simulation of SEU for SRAM cells. *J Semicond*, 2007, **28**: 138–141. (in Chinese) DOI: [10.3321/j.issn:0253-4177.2007.01.029](https://doi.org/10.3321/j.issn:0253-4177.2007.01.029)
- [19] Krawzenek D, Hsu P, Anthony H, *et al.* Single event effects and total ionizing dose results of a low voltage EEPROM. *IEEE Radiation Effects Data Workshop*, 2000, 64–67. DOI: [10.1109/REDW.2000.896271](https://doi.org/10.1109/REDW.2000.896271)